JOURNAL OF GEOPHYSICAL RESEARCH, VOL. 114, B07404, doi:10.1029/2008JB005950, 2009

A model for the termination of the Ryukyu subduction zone against Taiwan: A junction of collision, subduction/separation, and subduction boundaries

Francis T. Wu,[1] Wen-Tzong Liang,[2] Jian-Cheng Lee,[2] Harley Benz,[3] and Antonio Villasenor[4]

Received 23 July 2008; revised 19 February 2009; accepted 7 April 2009; published 11 July 2009.

[1] The NW moving Philippine Sea plate (PSP) collides with the Eurasian plate (EUP) in the vicinity of Taiwan, and at the same time, it subducts toward the north along SW Ryukyu. The Ryukyu subduction zone terminates against eastern Taiwan. While the Ryukyu Trench is a linear bathymetric low about 100 km east of Taiwan, closer to Taiwan, it cannot be clearly identified bathymetrically owing to the deformation related to the collision, making the location of the intersection of the Ryukyu with Taiwan difficult to decipher. We propose a model for this complex of boundaries on the basis of seismicity and 3-D velocity structures. In this model the intersection is placed at the latitude of about 23.7°N, placing the northern part of the Coastal Range on EUP. As PSP gets deeper along the subduction zone it collides with EUP on the Taiwan side only where they are in direct contact. Thus, the Eurasian plate on the Taiwan side is being pushed and compressed by the NW moving Philippine Sea plate, at increasing depth toward the north. Offshore of northeastern Taiwan the wedge-shaped EUP on top of the Ryukyu subducting plate is connected to the EUP on the Ryukyu side and coupled to the NW moving PSP by friction at the plate interface. The two sides of the EUP above the western end of the subduction zone are not subjected to the same forces, and a difference in motions can be expected. The deformation of Taiwan as revealed by continuous GPS measurements, geodetic movement along the east coast of Taiwan, and the formation of the Hoping Basin can be understood in terms of the proposed model.

Citation: Wu, F. T., W.-T. Liang, J.-C. Lee, H. Benz, and A. Villasenor (2009), A model for the termination of the Ryukyu subduction zone against Taiwan: A junction of collision, subduction/separation, and subduction boundaries, *J. Geophys. Res.*, *114*, B07404, doi:10.1029/2008JB005950.

1. Introduction

[2] That the Ryukyu subduction zone runs westward into and terminates against the Taiwan mountain belt is commonly agreed, but the geometry of the Philippine Sea plate (PSP) and the Eurasian plate (EUP) at this junction has been given various forms in the literature [*Angelier*, 1986; *Angelier et al.*, 1990; *Lu et al.*, 1995; *Deffontaines et al.*, 1997; *Lallemand et al.*, 1997; *Font et al.*, 2001; *Kao and Rau*, 1999; *Kao and Jian*, 2001; *Chen and Chen*, 2004; *Wu et al.*, 1997]. On the basis of different data sets and conceptual tectonic frameworks these investigators may choose among four plate configurations that differ mainly in their geometry near Taiwan (Figure 1). In most cases the boundaries were shown without much discussion. However, more accurate representation of the boundaries will be necessary for understanding the tectonics of northern Taiwan.

[3] All of the models of the boundaries are essentially the same from the western terminus of the bathymetrically well-defined Ryukyu Trench to about 50 km offshore of eastern Taiwan (121.95°E and 23.54°N, Figure 1). At this point the submarine Hualian Canyon, which begins in the Hoping Basin and follows a southeastward course, reaches the foot of the Ryukyu accretionary wedge. Three of the four models place at least a part of the plate boundary along the Hualian Canyon. In all these models the collision boundary of PSP with EUP on the Taiwan side is the Longitudinal Valley with or without an extension along the northeast coast of Taiwan, to connect to the Ryukyu "Trench," i.e., the Hualian Canyon. In the following, we shall distinguish the models by their eastern boundary.

[4] Model I (Figure 1b) extends along the canyon and the western side of the Hoping Basin toward Suao [e.g., *Lu et al.*, 1995; *Angelier et al.*, 1990]. Model II (Figure 1b) also follows the canyon, but ends at about 24.2°N on the east

[1]Department of Geological Sciences, State University of New York at Binghamton, Binghamton, New York, USA.
[2]Institute of Earth Sciences, Academia Sinica, Taipei, Taiwan.
[3]U.S. Geological Survey, Denver, Colorado, USA.
[4]Instituto de Ciencias de la Tierra "Jaume Almera," CSIC, Barcelona, Spain.

0148-0227/09/2008JB005950$09.00

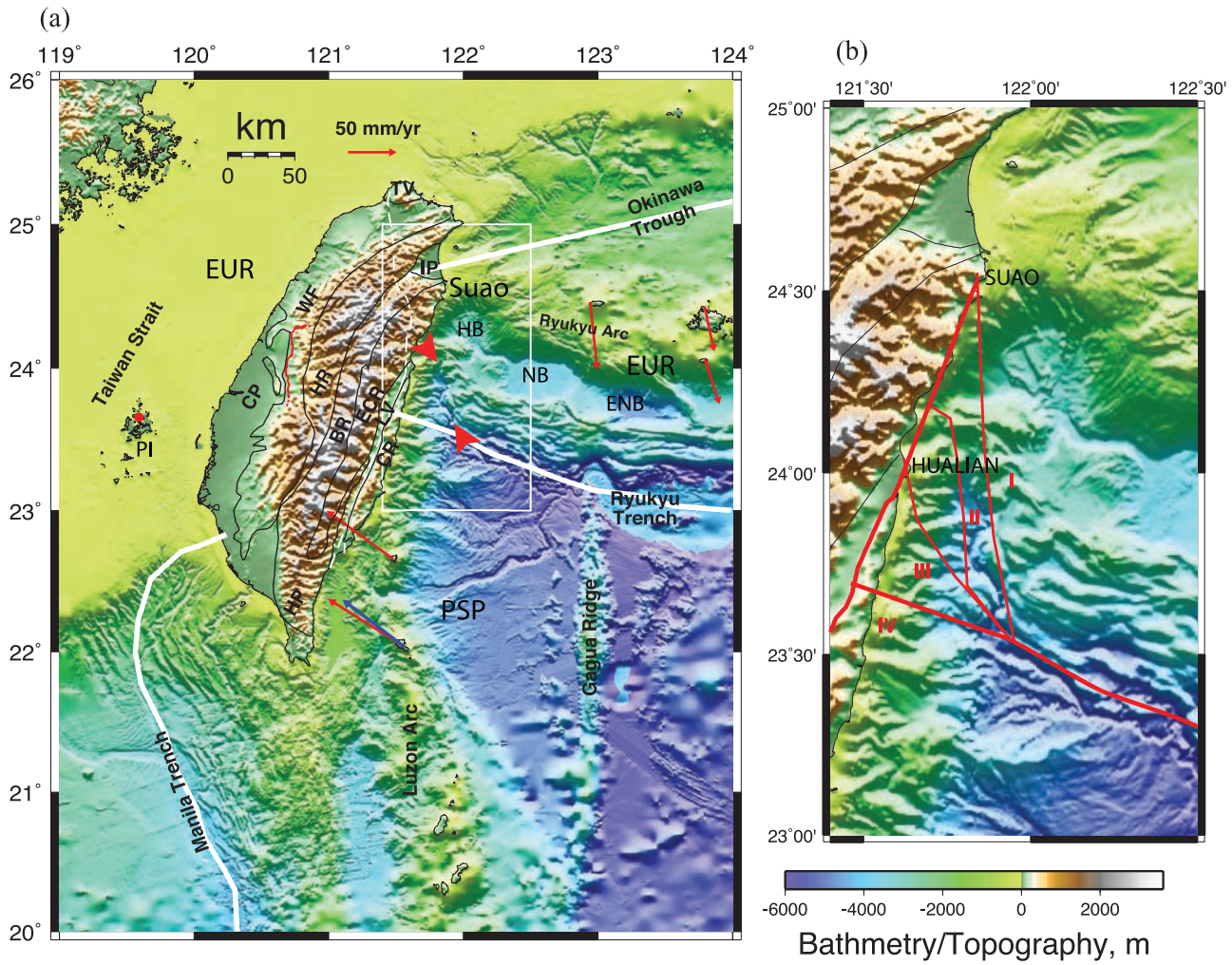

Figure 1. (a) Plate configuration in the vicinity of Taiwan. The arrows indicate the predicted (red, from NUVEL-1) and GPS-measured (blue, from *Yu et al.* [1997]) plate velocity vectors, relative to Penghu Islands (PI) with scale shown at top. (b) The four forms of junction referred to in the paper for the boxed area in Figure 1a. These are found in papers by different authors (see text). Between the two red arrowheads is the Hualian Canyon. The location of this area is shown by the white rectangle in Figure 1a. In this and Figures 2a, 3a, 6a, 6b, 8a, and 11, the frequently used place and geological province names are abbreviated. The place names are HB, Hoping Basin; IP, Ilan Plain; NB, Nanao basin; ENB, East Nanao basin; TV, Tatun volcano; and LV, Longitudinal Valley. The geological province names are CP, Coastal Plain; HR, Hsueshan Range; WF, Western Foothills; BR, Backbone Range; ECR, Eastern Central Range; CR, Coastal Range. Red line indicates Chelunpu Fault (of the 1999 Chi-Chi earthquake.) The less frequently used names can be found in the captions of the figures in which they appear.

coast of Taiwan [e.g., *Deffontaines et al.*, 1997; *Font et al.*, 2001]. *Kao et al.* [1998a] chose nearly the same boundary on the basis of the hypocentral distribution of local earthquakes and teleseismically relocated events offshore of eastern Taiwan. Model II is by far the most commonly used. In model III [e.g., *Lacombe et al.*, 2001], the boundary extends into Hualian (Figure 1b), at the northern end of the Longitudinal Valley; it is incorporated in one of the most commonly used 3-D representation of the plate tectonics of Taiwan [*Angelier*, 1986]. In all three of the models a piece of the Philippine Sea plate, explicitly identified as a part of the Luzon Arc by *Font et al.* [2001], is located offshore of northeastern Taiwan between the western and the eastern branches of the collision/subduction boundary. Thus, the Philippine Sea and the Eurasian plates (the Asian continental shelf locally) are in convergence there in this model [*Lallemand et al.*, 1997]. The eastern boundaries of these models are either a strike-slip fault [*Font et al.*, 2001] or not clearly specified. Model IV essentially extends the boundary along the discernible Trench westward, following the foot of the accretionary wedge, to meet the island; it is based on local catalog seismicity [e.g., *Wu et al.*, 1997]. The Ryukyu subduction boundary in this case intersects with Taiwan south of Hualian.

[5] To understand the effects of the collision of PSP with EUP, it is important to know the contact between the two

plates, and the exact geometry of the PSP subduction zone as it terminates against Taiwan becomes important. Except in model I above, in which the collision of the two plates occurs along the whole length of the Taiwan orogen from Suao southward, the other models involve the subduction of PSP northward north of the junction as it continues to move in the direction of N50°W to collide with EUP [*Seno*, 1977; *Yu et al.*, 1997]. The subduction of PSP means that the collision shall take place at increasingly greater depth to the north. Such a system is inherently three-dimensional, and it is the purpose of this paper to investigate the plate structures in the vicinity of the junction and to propose a 3-D model specifying the location of the junction. Although the plate boundaries at the surface are not clearly definable near Taiwan without a bathymetric trench, we can decipher the plate geometry using the two basic properties of an active subduction system: the seismicity associated with the subduction zone and its seismic velocity signatures. To resolve the seismic zones under northern Taiwan and its immediate vicinity more accurately, we use the well-tested method of double-difference hypocentral determination [*Waldhauser and Ellsworth*, 2000] and conduct a relatively high-resolution tomography under northern Taiwan to map 3-D velocity structures under northern Taiwan. Only events within the network or near the edge of the covered area are used in order to obtain good quality hypocentral solutions and velocity images. We use the results to construct a consistent plate model and then extrapolate to the surface to define the boundaries. Furthermore, to get a sense of the overall PSP subduction zone between the end of the well-defined Ryukyu Trench and eastern Taiwan, we combine data from the Ryukyu Islands and northern Taiwan to locate events in this area, again using the double-difference method [see also *Font et al.*, 2004; *Chou et al.*, 2006].

[6] The junction model so defined can be tested against other observations that are dependent on the plate geometry and kinematics. For example, at the intersection where the transition from collision to subduction occurs we can expect the stress regime to change along strike; while the change may not be abrupt it would be systematic. These changes could be detected either by changes in focal mechanisms of earthquakes or by deformation patterns as revealed by land-based GPS measurements. Also, if any part of the island overlies the junction, the interseismic deformation as measured by a leveling survey or GPS may undergo a change in behavior going from one side to the other and if the geometry of the termination has existed for an extended time, say more than 1 Ma, the topography may reflect this transition. The geometry of this boundary is certainly critical in the understanding of how the collision operates in Taiwan to create the mountains. Any attempt to geodynamically model the orogen must specify this boundary correctly.

[7] It should be noted that the model we shall propose is based on the present configuration of the Philippine Sea plate in northern Taiwan. This configuration may have existed for some time but in this paper we are not concerned generally about the time factor. There are many other models of Taiwan tectonics, such as those proposed by *Chemenda et al.* [2001], *Lallemand et al.* [2001], and *Sibuet et al.* [2002] that deal with evolutionary aspects of collision of Taiwan in the past millions to 15 Ma. It suffices to say that if the proposed model is correct, then the last stage of this model should be the same as the proposed model.

2. Seismicity and Tomography of Philippine Sea Plate Subduction Near Taiwan

2.1. Seismicity of NE Taiwan

[8] The double-difference earthquake relocation method [*Waldhauser and Ellsworth*, 2000] utilizes the differences of observed and calculated travel times for pairs of nearby events recorded at the same stations. It is the relative locations of clusters with respect to the average of all clustered events that are being solved. The advantage of the method is that the effects of three-dimensional velocity structures and possible clock bias (the time-invariant part) at different stations on event location are minimized. It allows the derivation of high-resolution seismicity in many areas [*Waldhauser and Ellsworth*, 2000]. While the relative arrival times at stations determined by cross-correlating the seismograms may bring the best results, even using catalog P and S times are found to sharpen seismicity [*Waldhauser and Ellsworth*, 2000], as confirmed by our previous work using the catalogs from Central Weather Bureau (CWB) of Taiwan [*Wu et al.*, 2004]. In this paper we apply the double-difference method to two data sets in order to determine the subduction structures under Taiwan and its eastern continuation. The first one is the 1994–2002 CWB P and S phase data and the other one is the phase data from the combined 1997–2003 Japan Meteorological Agency (JMA-NIED) and CWB data for events in the area between the east coast of Taiwan and the westernmost Ryukyu Islands, Japan (Figure 1). We have performed a massive reweighing of the arrival data based on the signal-to-noise ratio because, for operational reasons, the relatively small first arrivals from events in the northern inclined seismic zones were often down-weighed to achieve smaller RMS for hypocentral locations.

[9] In the map view (Figure 2a) increasingly deeper seismicity (color coded in Figure 2a) from south to north can be seen to lie under the north and northeastern part of the Taiwan Island. Although this fact has long been known [e.g., *Wu et al.*, 1997] the Wadati-Benioff zone (WBZ) is more sharply defined after the double-difference relocation. Although WBZ can be inferred from a seismicity map (Figure 2a) it is clearly displayed in the NNE oriented cross sections (Figure 2b). Close to the east coast of Taiwan, profiles 7–10 in Figure 2b show inclined zones distinctly below about 40 km. Above that depth complex structures in seismicity, most probably related to the brittle deformation of PSP, are found, rendering it impossible to determine where the seismic zone begins to bend, a feature one would associate with the initial downward flexure of a subducting plate. However, especially in profiles 8 and 9, along the Longitudinal Valley and the Coastal Range (see Figure 2a for the locations of the profiles), such points can be identified at the bottom of the zone (see arrows in the left part of the profiles). Using the scale on the profiles and referring to Figure 2a, we can estimate the intersection of the locus of the bending point with the Longitudinal Valley to be about 23.7°N (see Figure 2a and 2b, profiles 8, 9, and 10). The exact point of intersection at the surface is not physically meaningful but with the changes in boundary

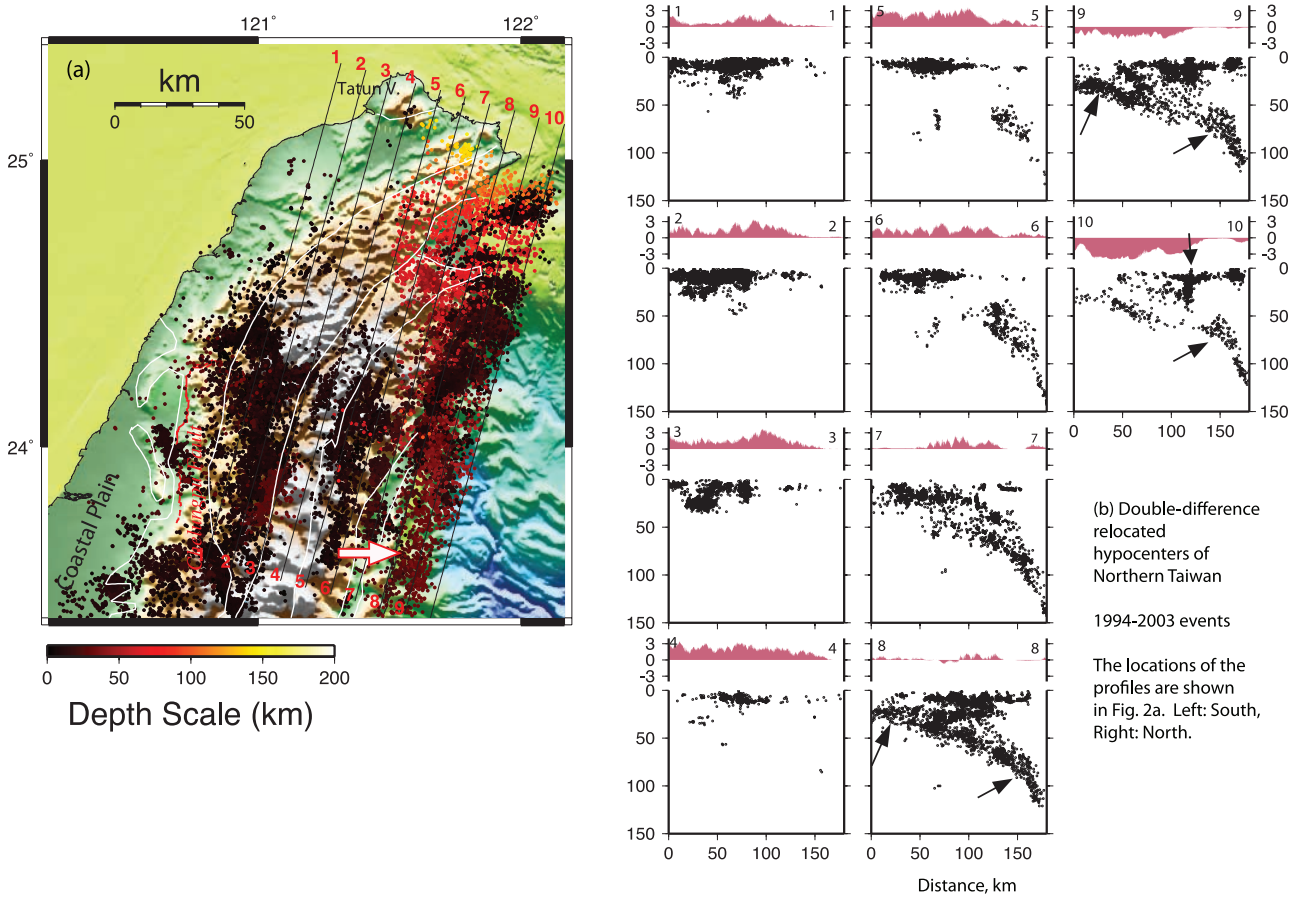

Figure 2. (a) Epicenters of relocated events 1994–2003. The dots are color-coded to show depth. The deeper events (as indicated by red and orange) underlying northeastern Taiwan define the surface projection of the inclined seismic zone. The zone extends under northern Taiwan as far as the Tatun volcanoes. (b) Cross sections along profile lines (10 km apart) in Figure 2a. Above each section the projected topography is drawn. Seismicity in profiles 1 through 4 in western Taiwan represents crustal events, mostly related to the 1999 Chi-Chi earthquake. In profile 5 the seismic zone shows activity only below 50 km, but in profiles 6 and 7 the shallower foci begin to fill in. But the zone does not become complete until profiles 8 and 9. In profiles 8 and 9 the bending of the bottom of the inclined seismic zone as marked by arrows can be used to mark the beginning of the dipping seismic zone. The corresponding location on the surface can be viewed as the place where the Philippine Sea plate begins to subduct under the Eurasian plate. The double-layered seismicity in the inclined seismic zone is clearly displayed in profiles 7 through 10. The separation of the two layers is about 15–20 km. Arrows on the right hand side of profiles 8, 9, and 10 indicate the point a noticeable bend in the seismic zone can be identified.

conditions around this point the deformation as revealed through GPS measurements, the focal mechanisms of earthquakes and the uplift rate along the eastern coast of Taiwan can be expected to vary significantly, as we shall show later.

[10] Along strike and toward the west the shallow seismicity under northern Taiwan is disconnected from the deeper (>50 km) zone as shown profiles 5 and 6 (Figure 2b). Farther westward, in profiles 1–4, seismicity is found only above 50 km. In terms of his systematic disappearance of the seismic zone below 50 km depicts the shape of the PSP at its western terminus, to be mapped in 3-D later. Incidentally, the very narrow, nearly vertical zone beneath the WBZ shown in profiles 5 and 6, at about 70 km on the horizontal axis has been known (S. Roecker, personal communication, 2004) but an adequate explanation is still elusive.

[11] To explore the geometry of the WBZ offshore of northeastern Taiwan, we relocated the seismicity in the region using events that have been recorded by both the CWB network and the Japanese seismic stations in SW Ryukyu (from Hi-net, NIED, Japan) (Figure 3a). Data from October 1997, through March 2003, are included. Because the stations are only on two sides of the roughly rectangular region, we do not expect the locations to be as precise as those within the CWB network. The relocation does result in tighter clusters and generally better defined seismic zone in this area. The epicentral distribution and the location of 11 profile lines are shown in Figure 3a and the corresponding profiles are shown in Figure 3b. Profile 1 (Figure 3b), a few kilometers to the east of profile 10 in Figure 2, and profile 2 show a bend in the deeper part of the WBZ. They demonstrate that the WBZ on both sides of NE Taiwan shoreline

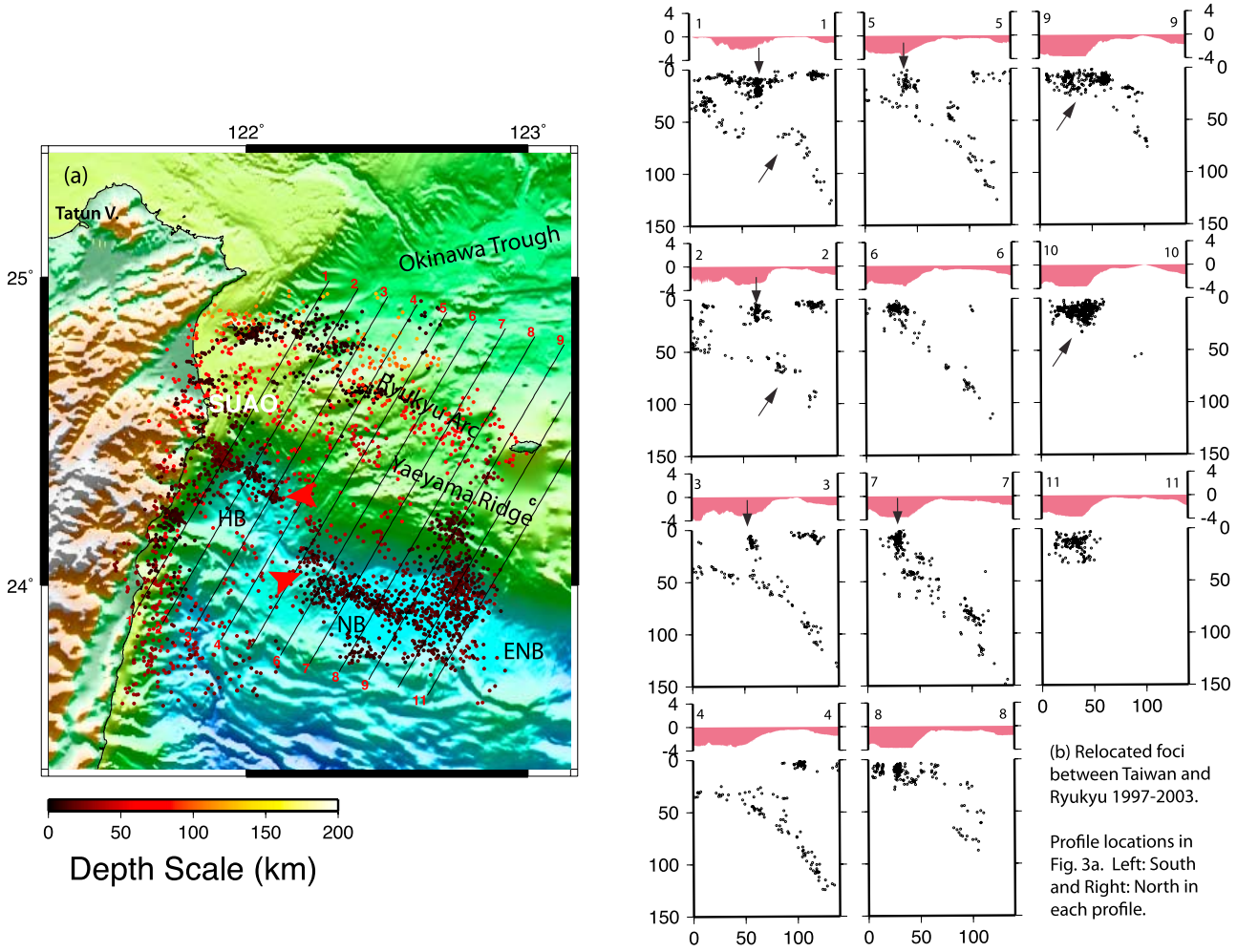

Figure 3. (a) Relocation of seismicity in the offshore area of NE Taiwan using 1997–2003 P and S phase data from the CWB stations in northern Taiwan and JMA-NIED stations in SW Ryukyu stations (JMA-NIED catalog). The two red arrowheads point to two linear zones of shallow seismicity that was a nearly continuous curved zone. See text for more details. (b) Corresponding cross sections. Long arrows in profiles 1 and 2 mark the locations of a bend in the seismic zones. Profile 1 is very close to profile 10 in Figure 2b. The arrows in profiles 9 and 10 point to the seismicity on the northwest side of the subducted Gagua Ridge (Figure 1a). The short vertical arrows in profiles 1, 2, 3, 5, and 7 indicated the near vertical seismic zones associated with the shallow seismicity in Figure 3. See caption for Figure 1a for abbreviated place names.

(see also profiles 8–10 in Figure 2b) has a kink at the depth of about 60 km. From profiles 3 onward the bend is no longer visible. This kink was shown by *Kao and Rau* [1999] under the NE coastal area of Taiwan and they interpret it as the point at which the sources of the subducted lithosphere change from crust to mantle. In the eastern part of this area (profiles 9–11) a very active N-S trending shallow seismicity belt under the Nanao ridge between the Nanao and East Nanao basins (NB and ENB in Figure 3a) [*Font et al.*, 2001] is seen. Noting that the Gagua ridge is located along the 123°E meridian and that PSP moves toward the northwest and this seismic belt is located to the northwest of tip of this ridge after it enters the Ryukyu Trench [*Dominguez et al.*, 1998], a causal relation among the seismic activity, the subduction of the ridge, and the formation of the ridge can be expected.

[12] The relocated offshore seismicity resolves finer structures in the seismic belt offshore of NE Taiwan. In the area between the NE coast of Taiwan and 123°E CWB earthquake locations show an arc-shaped shallow (0–10 km) seismicity belt [see *Kao et al.*, 1998a, Figures 2b and 3a] trending generally ESE. *Kao and Jian* [2001] subsequently used the curved belt as the PSP/EUP boundary in southwestern Ryukyu. After relocation, however, the events appear to divide into two nearly parallel segments along its length offset by about 30 km in WNW direction in the middle (Figure 3a). The offset coincides with a jog in the Ryukyu arc on the eastern side of the Hoping Basin. Both zones appear to be nearly vertical in cross sections, indicated in Figure 3b by short vertical arrows in profiles 1–3, 5 and 7, and they overlie the dipping seismic zone (at 40–50 km). Thus, these zones cannot be used to mark the boundary between PSP and EUP at the bottom of the ocean.

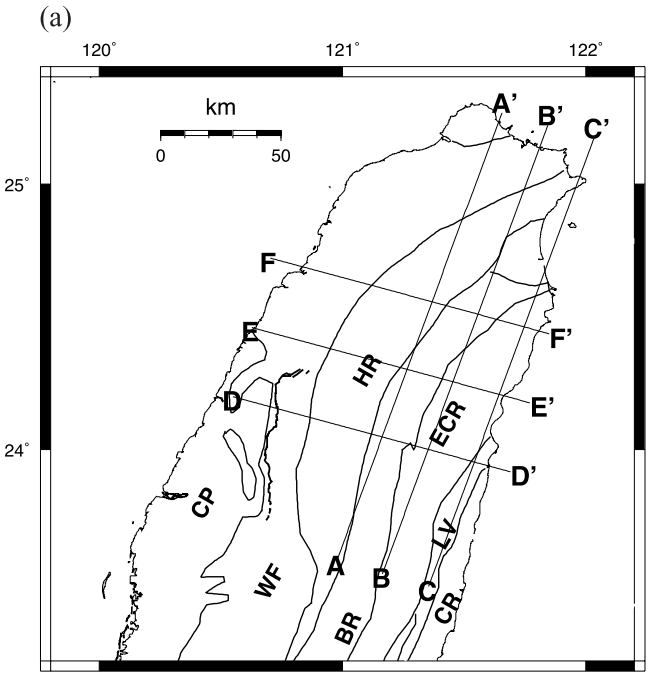

Figure 4. Tomographic sections in northern Taiwan. (a) Locations of the three N20°E and three S75°E sections. The plate boundaries are the same ones shown in Figure 1a. See the caption for Figure 1a for the names of the geological regions. (b) Corresponding N20°E tomographic sections AA′, BB′, and CC′. (c) Corresponding S75°E tomographic sections DD′, EE′, FF′; the red upright arrows show the approximate locations of PSP/EUR boundary. (left) The absolute P wave velocities and (right) dVp, the perturbation in percentage, from the 1-D initial model. In the Vp plots the contour intervals are 0.5 km/s. Above each section the topography along the profile is shown and below each section the color scale for Vp or dVp is shown. Notice that the same velocity scale is used for all Vp sections but in order to enhance resolution the ends of the rainbow scale is adjusted to show the maximum and minimum of each dVp section To assess the resolution of the sections results of checkerboard tests, see the results of checkerboard tests in the auxiliary material.

In Figure 3b there is a lack of events deeper than about 50 km in profiles10 and 11 due to the scarcity of events at deeper depths in the catalog used. From the profiles in Figure 3b it appears that the nearly E-W trend of the WBZ from 123°E westward is largely maintained, not turning sharply to the northwest as implied by models I, II, and III (Figure 1). Before we use the seismicity to construct the junction model we shall look at the 3-D velocity structures in this region.

2.2. Tomography

[13] It is well known [e.g., *Iidaka et al.*, 1992] that high-velocity anomalies (dVp > 0) are associated with subduction zones. Utilizing the same 1994–2002 CWB arrival time catalogs that we used for relocating seismicity, we can tomographically image the lateral variations in P velocities to provide additional constraints on the geometry of the PSP subduction zone and the crustal structures related to the subduction/collision. The tomographic algorithm of *Benz et al.* [1996] was used in this research. The velocity model of northern Taiwan consists of 42 × 86 × 77 (number of blocks in x, y, z directions) 5 × 5 × 2 (in x, y and z directions) km^3 blocks. For assessing the resolution of the tomographic results we present the results of checkerboard tests in the auxiliary material.[1] We shall concentrate our attention on the well-resolved features related to the northern Taiwan plate tectonics [see also *Rau and Wu*, 1995; *Y. Wu et al.*, 2007].

[14] Two series of tomographic cross sections are shown in Figures 4b and 4c and their locations are shown in Figure 4a. Those in Figure 4b (AA′ to CC′) are essentially in the dip direction of the northern Taiwan subducting slab and those in Figure 4c (DD′ to FF′) are perpendicular to the trend of the island. For each section in Figures 4b and 4c the absolute velocities, Vp, are shown on the left and the perturbations from the initial 1-D model, dVp, on the right; the white dots are hypocenters within 5 km of the section line. In Figure 4b, referring to the western limit of the PSP seismicity under northern Taiwan (shown as dashed line in Figure 4a), the AA′ profile overlies the area where only deep seismicity is present, BB′ includes the shallower portion and CC′ overlies the complete zone.

[15] In section CC′ (Figure 4b) the Vp > 8 km/s and dVp > 10% patches clearly form a dipping zone that follows the WBZ. Judging from the geometry of the curved anomalous zone in CC′, the subduction zone begins to dip at about 30 km from the south, essentially in agreement with our conclusion based only on inclined seismic zone. A sizable low-velocity anomaly can be observed above the subduction zone under the Ilan Plain (center ~130 km from the left in the dVp plot), the western extension of the actively spreading Okinawa Trough. In section BB′, located near the ridge of the Central Range, the seismicity is low above 40 km but below that depth both seismicity and the high Vp (8 km/s) or the large positive dVp (10%) zones are well-defined and coincide. The extent of crustal root under the high Central Range can be seen by tracing the 7.5 km/s contour in the Vp and viewing the dVp less than 5% patches in section BB′. In section AA′, located mostly between the Hsueshan Range Foothills and the Central Range, the crustal low velocity is less extensive than in BB′ and the high-velocity zone enclosed by the 8 km/s contour shows the deeper part of the subduction zone. The high Vp (8 km/s) zone is deeper than 60 km.

[16] In Figure 4c the three sections are perpendicular to those in Figure 4b. The 7.5 km/s contours in each section deepens toward the east under western Taiwan (Figure 4c (left) for DD′ to FF′) to attain the greatest depth under the higher Central Range. It then shoals toward the east, much more rapidly than the deepening on the west, thus forming a highly asymmetric root. Although the Moho velocity under Taiwan is yet not determined with confidence, using the 7.5 km/s contour as a guide we see that the crust is thickest along DD′ and gets thinner toward the north. Viewing the dVp plots in Figure 4c, the low-velocity anomalies form the core under the Central Range and on its east side (especially

[1] Auxiliary materials are available in the HTML. doi:10.1029/2008JB005950.

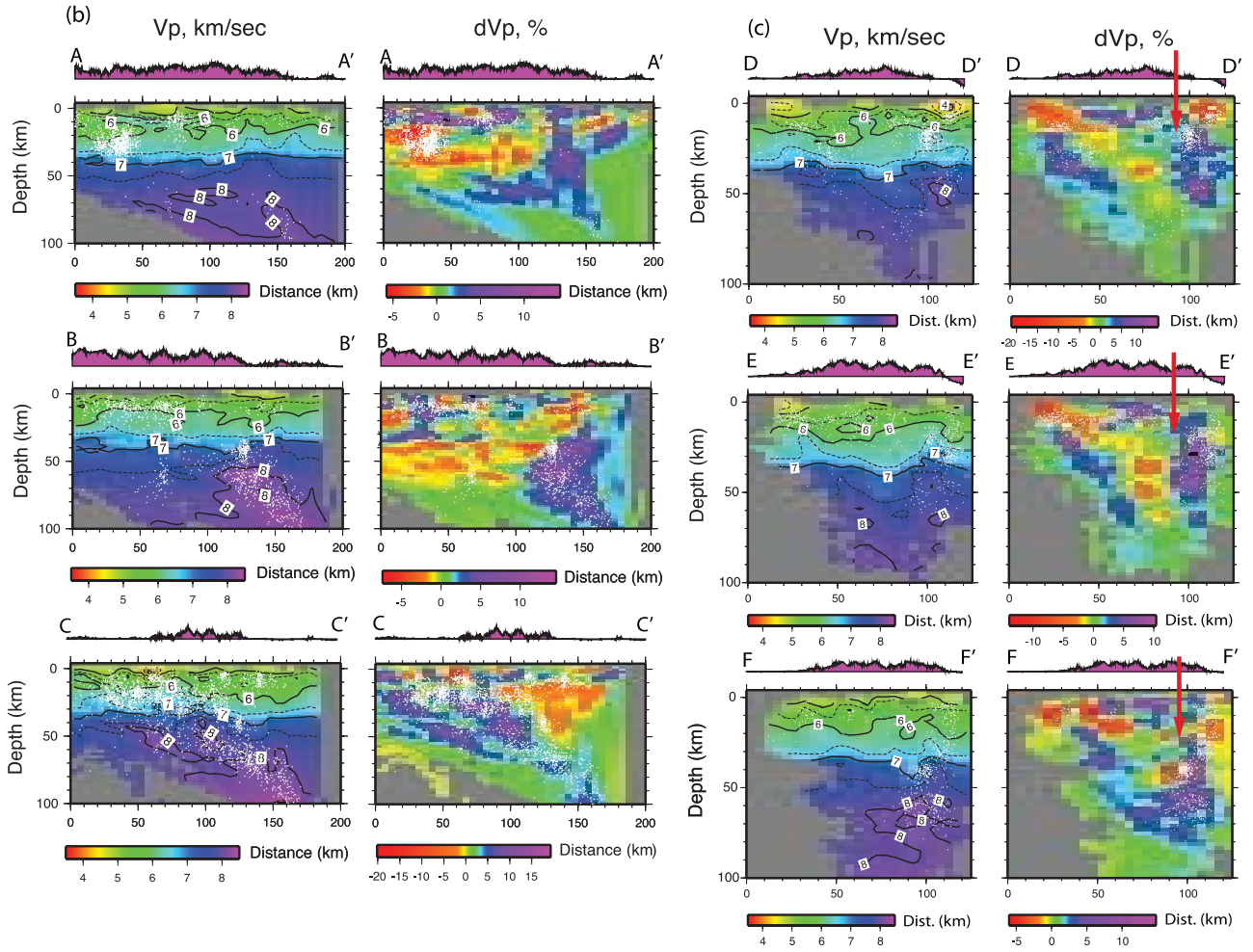

Figure 4. (continued)

in profiles DD′ and EE′) this core abuts on a high-velocity zone (marked by the vertical arrow), apparently the western edge of the PSP. In FF′ the high/low boundary is not as well defined at depth above ~20 km, but at greater depth it is clear. The easternmost part of this section is underlain by a clear low-velocity zone in the upper 25 km, probably a part of the Hoping Basin [*Hetland and Wu*, 2001; *McIntosh et al.*, 2005]; because it is very close to the east coast of Taiwan, where there are few seismic stations, it is not well resolved. The Vp > 8 km/s or dVp > 10% region below 50 km in FF′ coincides with the high-seismicity zone; it is apparently the western end of the subducting PSP. The EUP/PSP boundary, as represented by the contact between the low and high velocities under the eastern Central Range, successively goes farther westward as shown by the arrows in DD′ through FF′. Using both seismicity and the seismic P velocity we can define the subducting collision boundary.

3. A 3-D Model of the Subduction of Philippine Sea Plate Near Taiwan

3.1. Basic Model

[17] On the basis of the seismicity and tomographic cross sections above and interpreting the WBZ and the concomitant relatively high velocity zones as plates we present the following tectonic model for northern Taiwan. We note first that plate boundaries are usually described as lines on a map, i.e., they are expressed in two dimensions. However, because the PSP terminates against Taiwan, simultaneously colliding with it and subducting northward, to appropriately understand the effect of collision along the collision/subducting boundary the geometry of the junction must be described in 3-D. The main elements of the proposed model are shown in 2-D in Figure 1a. The PSP begins to subduct northward under EUP at the foot of the Ryukyu accretionary wedge and the subduction zone intersects Taiwan at the latitude of about 23.7°N. Simultaneously, the N75°W component of the NW moving PSP resulted in the collision of PSP with EUP and mountain building in Taiwan. However, because of the PSP subduction the collision varies along the collision boundary. To the south of the junction, PSP and EUP are in full contact from surface down, but toward the north the two are in collisional contact only at increasing depth, following the deepening subduction zone. To illustrate the 3-D aspects more clearly, we provide several perspective views of the plate architecture under northern Taiwan in Figure 5. The subduction zone in Figure 5 is represented by the top and bottom surfaces that sandwich the dipping SW Ryukyu seismic zone. In the view from above, the western edge of PSP is inserted under northern Taiwan where the point "1" shows the point of intersection of LV with the PSP/EUP boundary, the point "2" is the

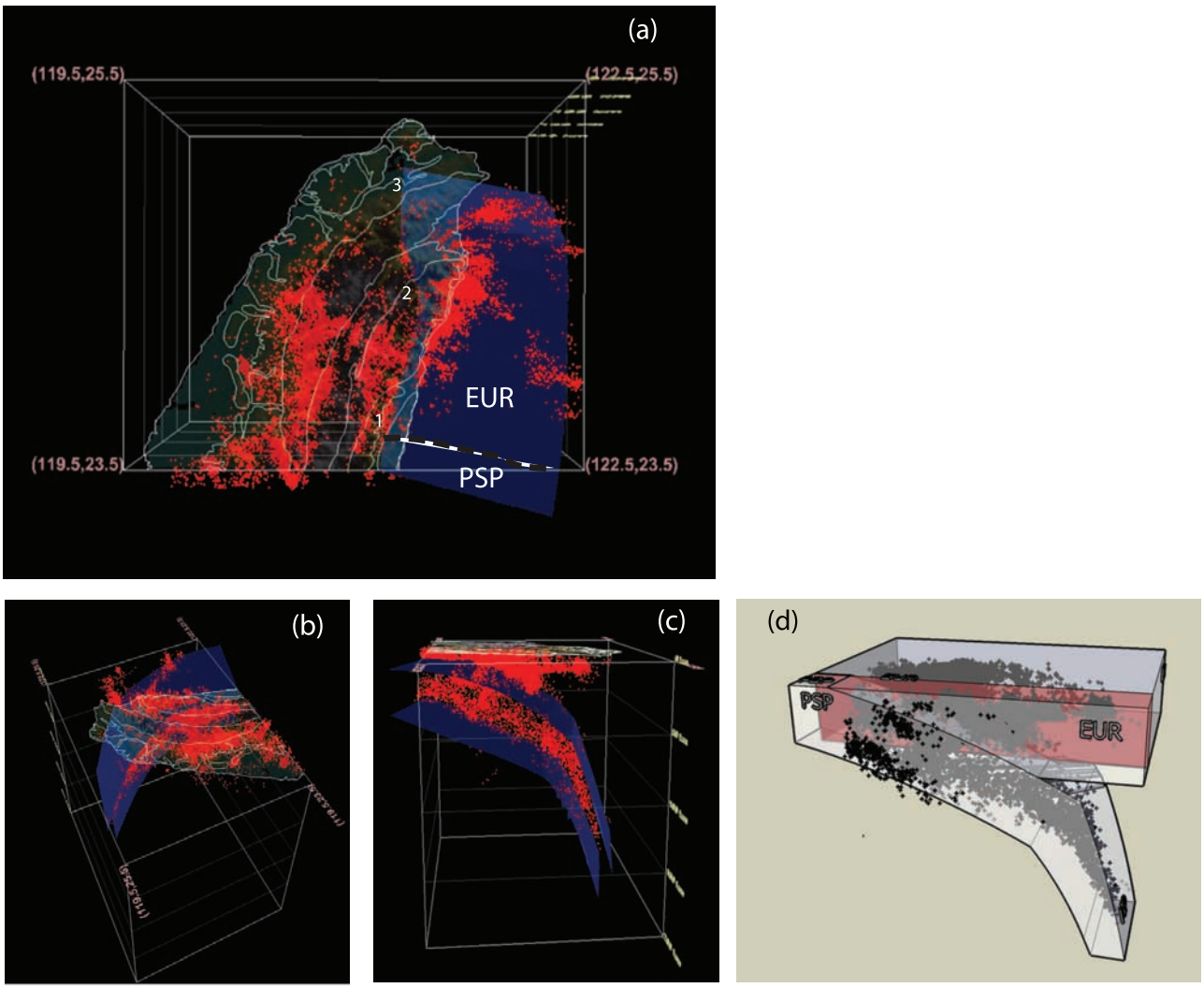

Figure 5. Perspective views of seismicity and our plate tectonic model of northern Taiwan. The 3-D ArcScene (ESRI/GIS) plots (Figures 4a–5c) and a Google Sketchup rendition of the block structures (Figure 5d). In Figures 5a–5c the upper and lower surfaces of the northern subduction zone are constructed to contain most of the dipping seismic zone in between them and conform to the Vp velocity model from tomography. (a) A view of the top of the model showing the outline of northern Taiwan, geologic provinces and the plate boundary between PSP and EUP. The boundary follows the Longitudinal Valley, and the PSP/EUR subduction boundary is located south of Hualian. To the north of this junction, PSP submerges because of its subduction, and the WNW motion of the PSP collides with EUR at successively deeper depth going north. EUR sits astride and above the boundary. After PSP enters the asthenosphere under northern Taiwan the westward motion of the PSP resumes and thereby creates a curved edge at the western end of PSP (as indicated by numbers 1, 2 and 3 in map view). (b) Viewing the Ryukyu subduction zone from the east. (c) A view above from the northwest. See Animation S1 in the auxiliary materials for more detail. (d) View from the northeast of the subduction and collision of PSP and EUR collision.

location where PSP enters the asthenosphere (at about 50 km), and the point "3" is under the Tatun volcanoes (Figure 1b). Figure 5b shows the NW view and Figure 5c shows the view from the east. In the online Auxiliary Materials, two animated views of the model from different angles are displayed.

[18] The idealized junction is located in the Longitudinal Valley, which has been identified as the high-angle contact between PSP and EUP [*Wu et al.*, 1997]. North of the junction, EUP straddles the subducting collision boundary. In this model the Coastal Range north of 23.7°N is currently situated on the subducting PSP. With PSP moving at ~80 mm/a in the direction of N50°W and the plate boundary trending N15°E, a convergence of more than 70 mm/a is expected. However, with the colliding/subducting PSP, the contact of PSP and EUP on the Taiwan side gets deeper as shown in Figures 5c and 5d. In Figure 5d the red-tinted plane marks the collision/subduction boundary; to the

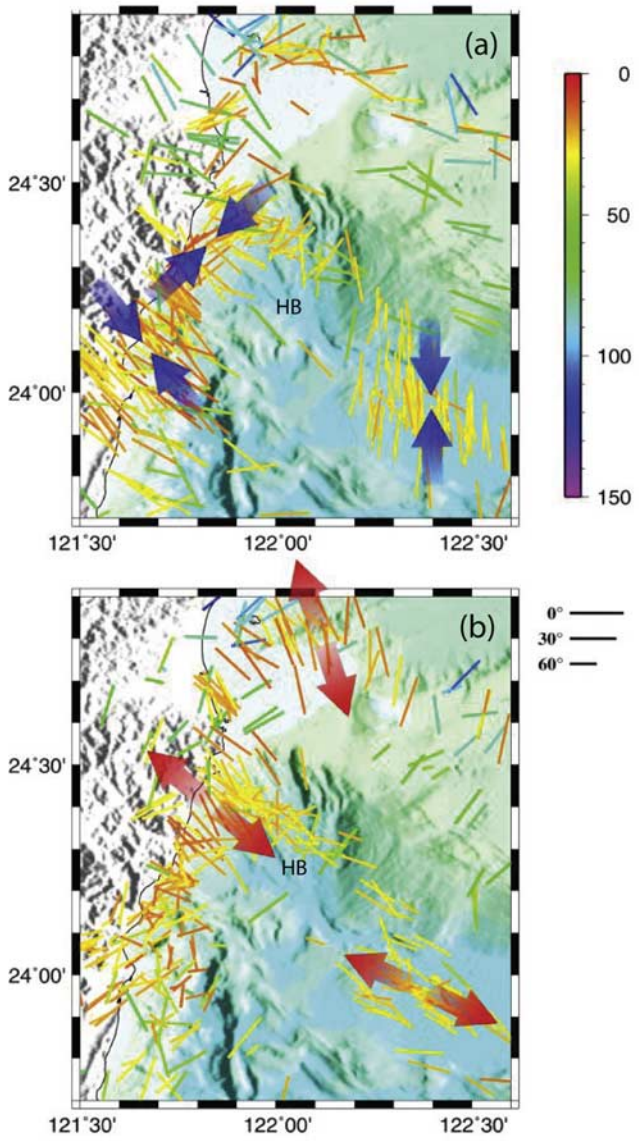

Figure 6. Seismic stress pattern derived from the BATS CMT Solutions (1995–2004, http://bats.earth.sinica.edu.tw) (a) Direction of P axes. (b) Direction of T axes. The bar length indicates the plunge angle of the stress axis, whereas the rainbow color indicates the corresponding focal depth. Note that a change of dominant NW-SE P axis to NW-SE T axis for shallow (<35 km) events occurs around 24.3°N along the coast (see text).

left (south) the PSP and EUP are colliding from the surface down, but to the right EUP is colliding with the PSP at increasing depth as the PSP subducts. As a result the EUP on the Taiwan side is compressed, albeit at increasing depth, but on the Ryukyu side the EUP is not being compressed and is coupled to the NW moving PSP only by friction at the interface. Thus, the EUP above the subducting PSP at the contact may be subjected to WNW-ESE tension due to the difference of motions on the two sides. Toward the north the compression on the Taiwan side gradually diminishes and leads to the tapering off of Central Range and the formation of a structural bight in the Tanao schist of northeastern Taiwan [*Ho*, 1988]. Once PSP goes below the lithosphere it apparently can move westward as shown in Figures 1b and 5a.

[19] There is another structure that adds to the complexity of this junction, namely, the Okinawa Trough behind the Ryukyu Islands (Figure 1). The recent phase of the opening of southwestern Okinawa Trough near Taiwan began about 2 Ma ago and had a total horizontal opening of about 30 km [*Sibuet et al.*, 1998]. As a result of the opening, the Ryukyu trench has migrated to the south. Recent GPS monitoring in Ryukyu and Taiwan [*Nakamura*, 2004; K. Segawa et al., A block-fault model for GPS velocity field in Taiwan and the Ryukyu Arc, paper presented at AOGS 3rd Annual General Assembly, Asia Oceania Geoscience Society, Singapore, 2006] indicates that the rate of relative motion between Taiwan and southern Ryukyu may be as high as 5–6 cm/a (Figure 1), much higher than the estimated rate (~1.5 cm/a) of the opening of Okinawa Trough in the last 2 Ma [*Sibuet et al.*, 1998]. In any case, the opening of the Okinawa Trough would lead to the migration of Ryukyu Trench southward with respect to fixed EUP, and most probably the point at which it intersects with the LV will migrate southward too. For convenience, we shall refer to this model as the subducting indenter model.

3.2. Implications for the Tectonics of Taiwan

[20] The subducting indenter model of northern Taiwan described above has several immediate implications. First, the change from full collision at the surface to partial collision at increasing depth along the collision boundary as described above might be expected to lead to a change in the states of stress along the boundary. South of the junction we expect the domination of thrust type mechanisms with P axis subparallel to the plate motion vector, while to the north the mechanisms above the subducting plate should gradually change to a mixture of normal and strike-slip events with T axis in the WNW-ESE direction; where PSP is in contact directly with EUP the thrust type would still dominate. Second, if this tension has operated for an extended period, then extensional structures offshore of northeastern coast may have been created. Third, the 3-D plate configuration determines also the overall deformation field in northern Taiwan as measured by GPS. In the long term such variations would affect the geologic structures. But because the rate of convergence is high enough the short-term deformation pattern can be used to discriminate the plate models shown in the box in Figure 1a.

[21] In addition, the location of the PSP-EUP junction places the northern part of the Coastal Range over the shallow part of the PSP subduction zone. Because of the continued spreading of the southern Okinawa Trough, the junction may move southward and lead to increased load on the plate and therefore more flexure. Under such circumstances we can expect the northern part of the Coastal Range to rise much slower than the southern part. Besides its effect on the long-term uplift of the Coastal Range, as judged by its topography, and the effect of the southward migration of the subduction boundary may also be seen in the leveling data.

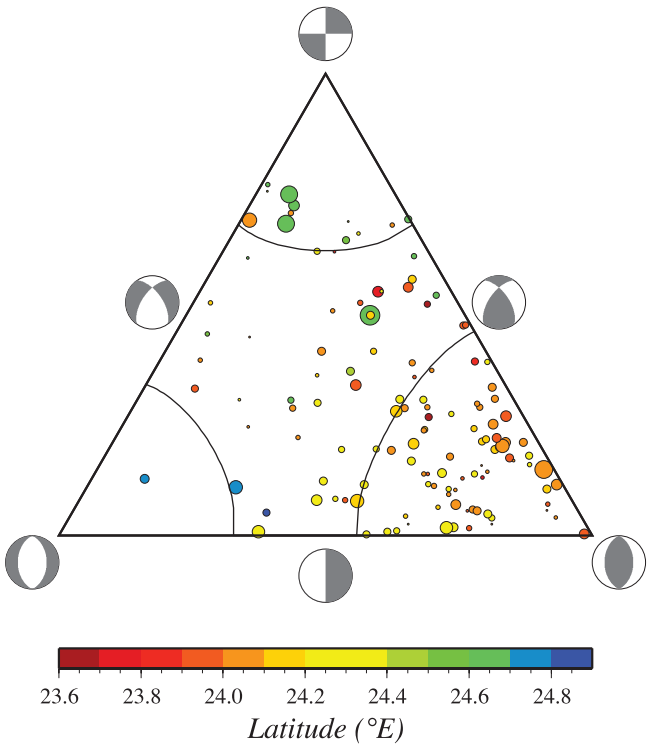

Figure 7. Ternary diagram for BATS focal mechanisms of shallow earthquakes for relocated epicenters using HypoDD. The symbol size is proportional to the moment magnitude. The color for the symbol denotes the latitude for each focal mechanism using the scale below. South of 24.3°N, reverse faulting dominates, and north of this latitude, normal and strike-slip events, especially at shallow depths (<35 km), are common.

[22] In section 4 we consider several observations against which we can compare our model predictions.

4. Model and Related Observations

[23] To see whether the tectonic implications of the subducting indenter model above agree with the observations, we check the model against changes in stresses as revealed by focal mechanism and GPS velocities along the collision/separation boundary, as well as longer term geological features such as topography of the Coastal Range and offshore structures in NE Taiwan.

4.1. Changing Stresses Onshore and Offshore of NE Taiwan

[24] The Broadband Array in Taiwan for Seismology (BATS) began operation in 1995 and has been used in moment tensor inversion for Mw > 3.5 events in the vicinity of Taiwan (see *Kao et al.* [1998b] and *Liang et al.* [2004] for introduction and the Web site http://bats.earth.sinica.edu.tw/for recent results). Although most of the events of interest in the present work are around the edge or outside of the network, the solutions have been shown to be robust [*Kao et al.*, 1998b].

[25] *Kao et al.* [1998a] mapped shallow dipping thrust events with P axis nearly perpendicular to the trend of the Ryukyu arc dominate in the area of Nanao basin and the wedge the area and deeper (>50 km) downdip extension events are evidently related to the subduction of the Philippine Sea plate. They also found an abundance of thrust faulting events, with P axes subparallel to the PSP motion vector, near the east coast of Taiwan they are related to the collision of PSP with Taiwan. However, as more BATS mechanisms of moderate size earthquakes become available a more complex pattern emerges. In Figure 6a we show the P axes and the T axes from a series of Mw 3.5–5.5 events. Of particularly interest is the south-to-north change in stress patterns for events near shore of NE Taiwan. For events above about 30 km, note the change near Hoping Basin (24.3°N; Figures 1 and 6a) of the P axes from NW to NE and the T axes from somewhat chaotic pattern to aligned WNW directions. The changing focal mechanisms along the collision/subduction boundary (Figure 6b) can also be viewed using the ternary diagram in Figure 7 [*Frohlich*, 2001]. Figure 7 shows that events south of 24.3°N concentrate in the lower right of the ternary diagram, indicating the dominance of thrust-type behavior, while north of that latitude normal and strike-slip faulting events begin to dominate.

[26] The changes in P and T axes patterns for shallow events shown in Figure 6 together with the changes in focal mechanisms revealed in Figure 7 are consistent with the change from WNW compression stress to NWW tension stress as the PSP subducts to greater depths. Note that in Figures 6a and 6b, events deeper than about 40 km still exhibit mainly WNW compression [*Kao et al.*, 1998a].

4.2. Surface Deformation From GPS

[27] The increase in the number of continuous GPS recording stations in Taiwan after the 1999 Chi-Chi earthquake enables the mapping of surface deformation of the whole island with higher spatial resolution. The horizontal velocity field of 2004–2007 in northern Taiwan, relative to the Paisha Island in Penghu, is shown in Figure 8 [*F. Wu et al.*, 2007; *Hsu et al.*, 2009]. This field records the short-term deformation of the orogen under the current boundary conditions. The results confirm the major key observations from previous GPS campaign data of 1991–1999 [e.g., *Yu and Kuo*, 2001]. Thus, the patterns of large velocities on the east coast of the Coastal Range, the rapid decay across the LV, the rapid decay in northern Coastal Range, the large and WSW directed velocities in southern Taiwan and very small velocities in the Coastal Plain are all clearly displayed. With the continuous data the velocity determinations are certainly more robust and the data in some parts of Taiwan, especially in northern Taiwan, where the field is now better described with more stations in the higher elevation and along the northeast coast. Four characteristics of the displacement field in northern and central Taiwan are particularly relevant to the model presented here.

[28] 1. There is a rapid decrease in velocities in the northern Coastal Range north of the region where we place the PSP-EUP junction. As shown in Figure 8a the velocities decrease moving from south to north, even though the directions of the vectors do not change significantly. When plotted against the distance from the southern end of the Longitudinal Valley (Figure 8b) the sharp decrease of velocities north of the100 km mark can readily be seen.

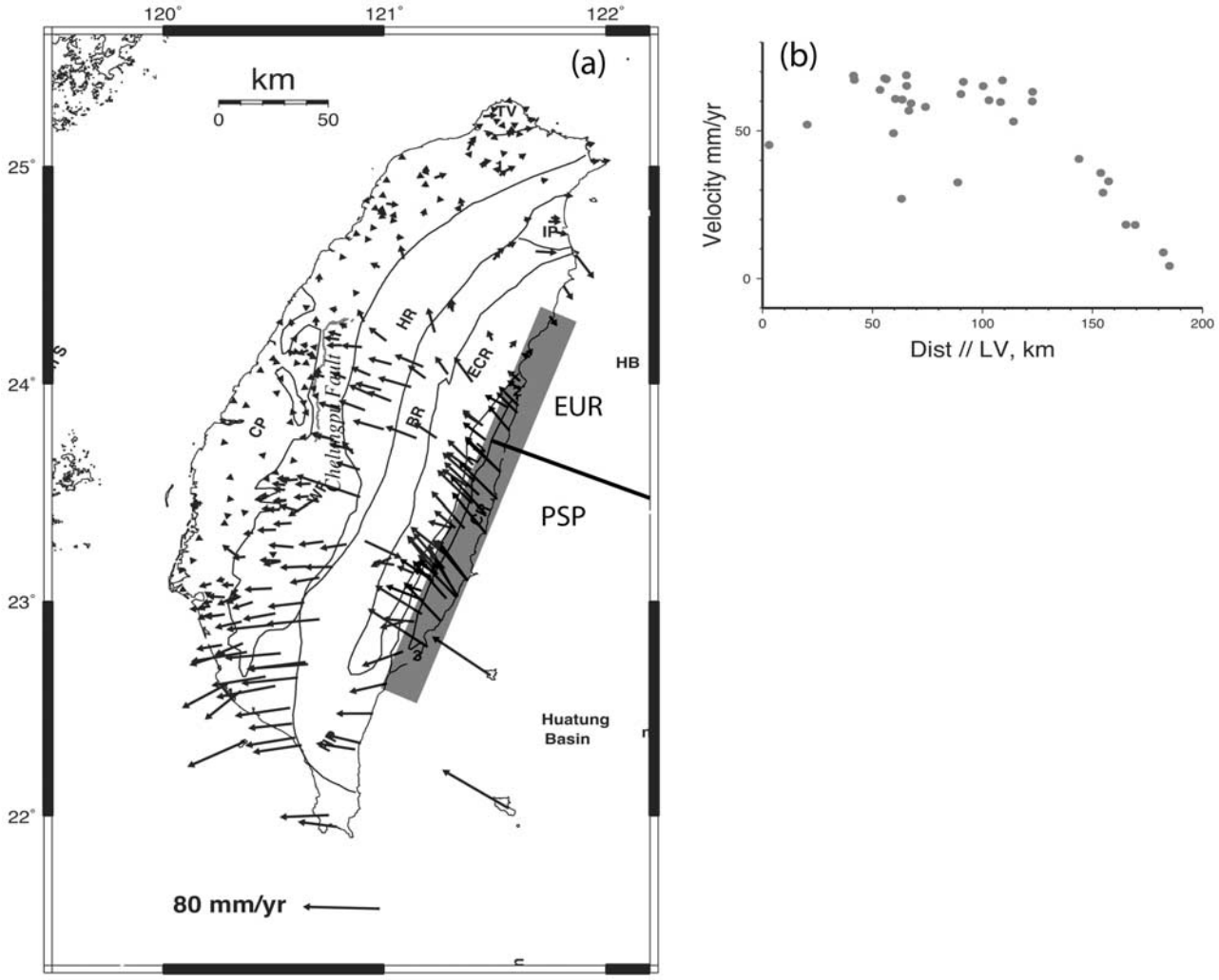

Figure 8. (a) Velocity vector field for 2004–2007 from continuous GPS measurements. (b) The change in the magnitude of GPS velocities as a function of distance along the LV. The area from which the data are taken is shown in Figure 8a as an opaque swath.

[29] 2. A systematic clockwise rotation of velocity vectors in the Coastal Range with respect to those in the Central Range and farther west can be discerned (Figure 8a).

[30] 3. Along the northeast coast of Taiwan the velocity vectors turn to SE directions (Figure 8a). The change from westward to eastward motion generally highlights the change of boundary conditions of the subducting indenter.

[31] 4. The velocity vectors in northern Taiwan north of about 24°N shows a clockwise rotation and a decrease in amplitudes with respect to those in the Coastal Range (Figure 8a).

[32] To model the GPS results fully is beyond the scope of the present paper, but whether the subducting indenter model is consistent with the geodetic observations just described needs to be explored. We use a simplified 3-D tectonic architecture as sketched in Figure 9a, taking into account of our indenter geometry. In the model, the indenter advances against the ''Eurasian'' block with the PSP motion. We used the commonly available package ANSYS, a finite element code http://www.ansys.com), for the calculation. The displacement conditions imposed on the boundaries are: all free except the west side is fixed, the bottom side does not move in the vertical direction and the east side is the collision/subduction boundary. The collision boundary (highlighted in blue in Figure 9a) is a fault with its friction coefficient varied for our simulation. In Figure 9b, results for fc = 0.1 and fc = 0.3 are shown. The main difference between them are that for fc = 0.1 the predicted (green) and observed (black) vectors on east side of the LV agree better; the directions of the vectors on the west side (red for the calculated values) do not change significantly with different fc values. Thus, conditions 1 and 2 can be modeled, and we conclude that a relatively low friction coefficient of 0.1 is appropriate. Although in the simulation there is a hint of clockwise rotation in northwestern Taiwan, our model fails to account for the large vector rotation in central Taiwan just north of 24°N (Figure 9b) as well as the southeastward motion on the northeast coast of Taiwan. The model predicts small westward motion of the eastern edge of the model even beyond the PSP/EUP junction as would be expected, since no other forces are available to push it eastward in our model. The modeling of the southeastward motion will probably require the model to be viscoelastic.

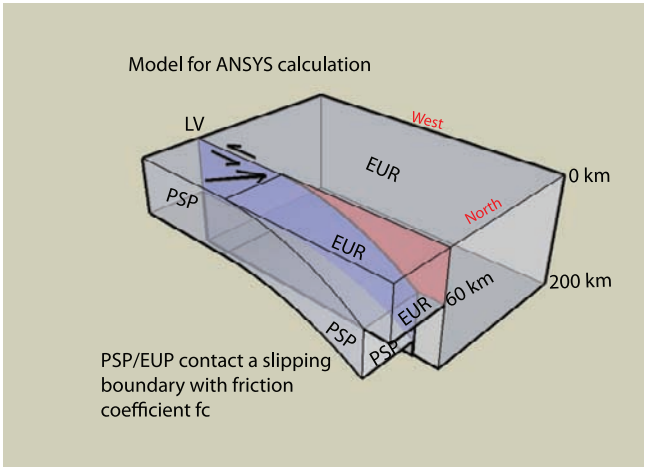

Figure 9a. A simplified subducting indenter model of PSP and Taiwan. The blue area on the interface between PSP and EUR is directly impacted by the collision. Above the deepening subducting boundary the area may be subjected to tension. See text for more details.

[33] *Hu et al.* [1997] used elastic 2-D models for earlier campaign GPS data; the entire Coastal Range was simulated as the indenter. *Rau et al.* [2008] modeled the northern Taiwan GPS observations in terms of several rotating elastic blocks. Although by no means exact our model demonstrates that the overall velocity field for a subducting indenter can explain the decrease of velocities along the LV. Condition 3 may arise from extrusion of northern Taiwan [*Angelier et al.*, 2009] when compressed from below, and if true, then a viscoelastic model is needed.

4.3. Topography and Leveling Survey Along the East Side of the Coastal Range

[34] Leveling surveys have been conducted repeatedly along the coast on the east side of the Coastal Range [*Liu and Yu*, 1990; C. C. Liu, personal communication, 2006]. Although the absolute value of the calculated rate of uplift is based on the tide gage values at Fugang near Taitung, with a precision of about ±10 mm/a, the precision of the relative rate along the surveying route is about ±3 mm/a (C. C. Liu, personal communications, 2006). The results of leveling (Figure 10) indicate that uplift is faster south of Shihtiping, in the middle section of the range, and it decreases sharply to the north. The longer-term uplift rates derived from the dating of uplifted marine terraces along the coast [*Liew et al.*, 1993; *Hsieh et al.*, 2004; *Yamaguchi and Ota*, 2004] range from ∼ 3 mm/a in the north to >10 mm/a in the south. The variations in the coastal uplift rate generally echo the low to high pattern of leveling data albeit the values do not match. The significance of the differences in the magnitude of uplift of these two data sets can be argued but evidently

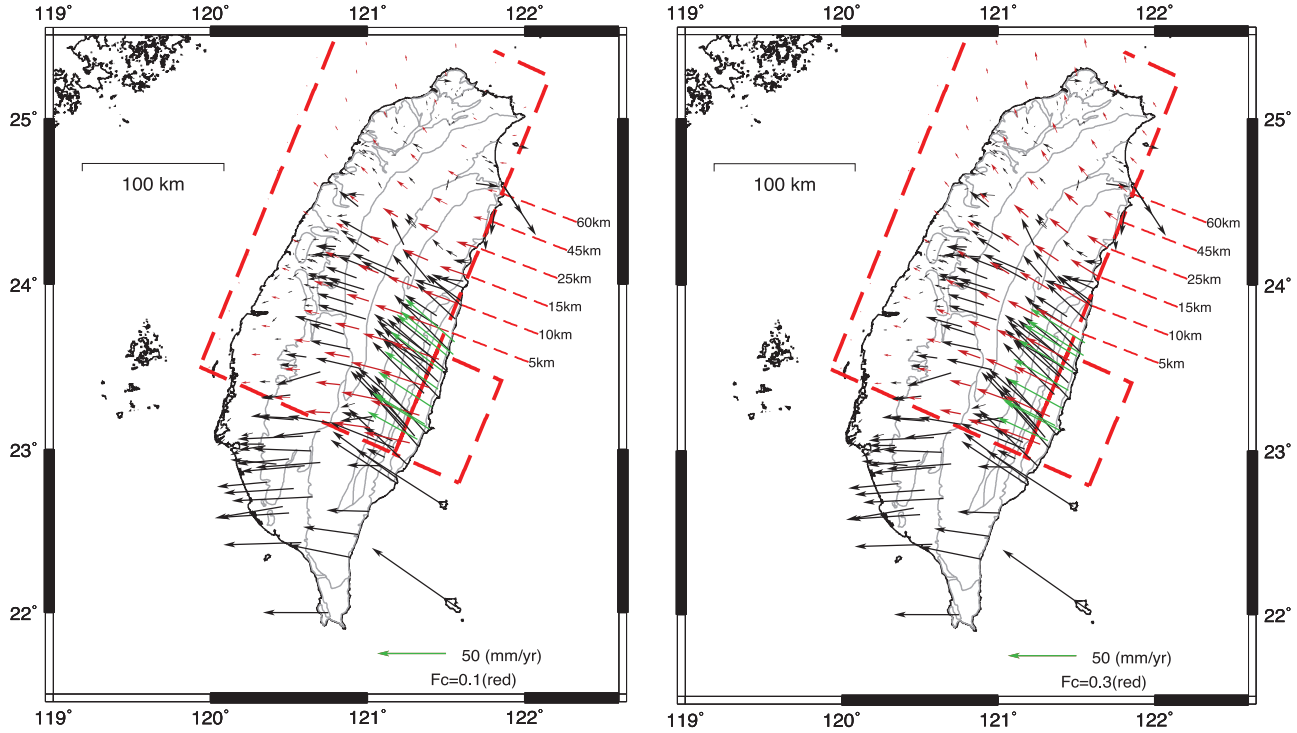

Figure 9b. Results of numerical simulation for a simple 3-D elastic model using the geometry of Figure 9a. The thick dashed lines outline the rectangular Taiwan block and the "PSP indenter." The Taiwan block is 200 km thick, and the tapering indenter is 50 km thick; numbers attached to the dashed line segments indicates the depths of the top of the "subducting indenter." The boundary conditions imposed are fixed western boundary and no vertical motion of the bottom of the model and the indenter moves at 80 mm/a toward N52°W, i.e., the relative motion EUP and PSP. The boundary between the indenter and the block, the blue plane in Figure 9a, is a frictional one with coefficient fc: (left) fc = 0.1 and (right) fc = 0.3.

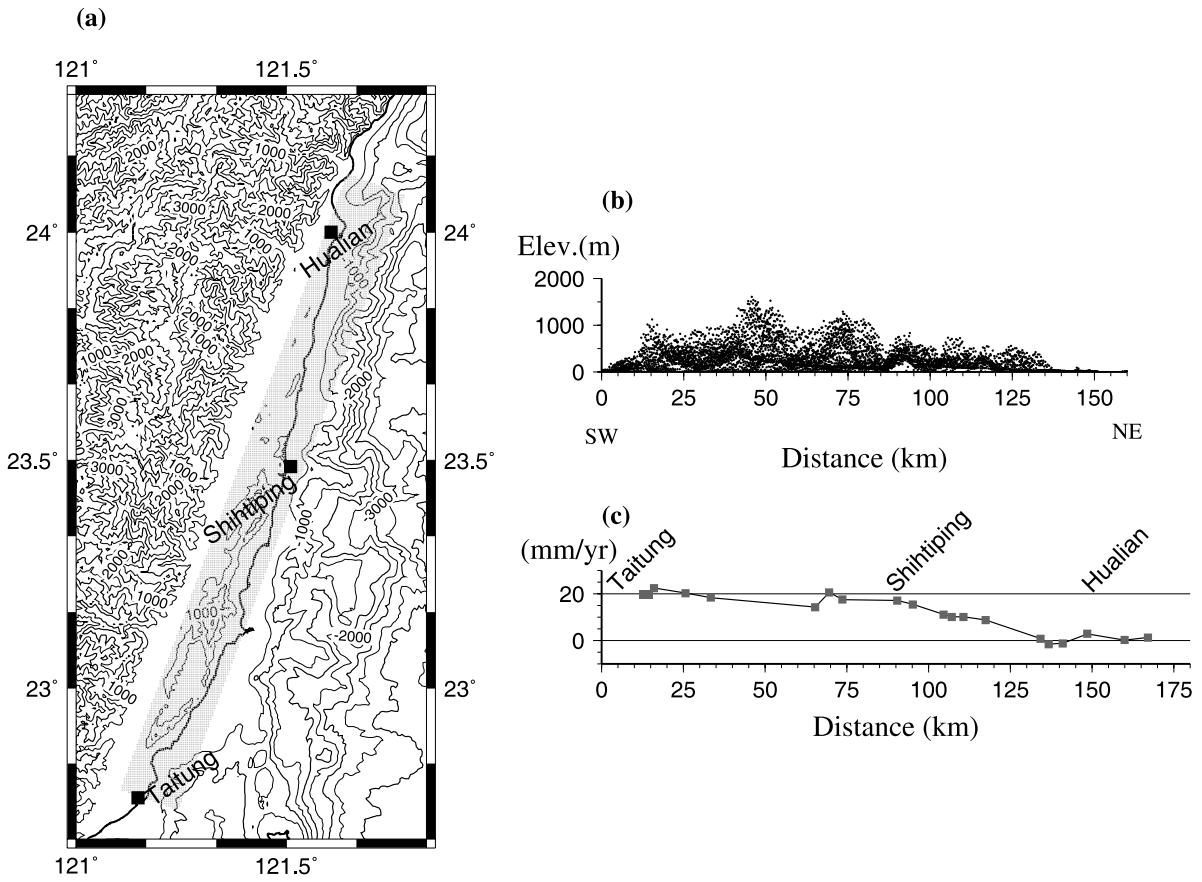

Figure 10. (a) A map of eastern Taiwan with the Coastal Range shaded. (b) The topography of the Coastal Range projected onto a line parallel to the Coastal Range. (c) Leveling data along the east coast of Taiwan between 1985 and 2001. The general shapes of the curves are similar, suggesting that the short-term and long-term processes that produce the data may be similar.

difficult to settle; a time-dependent rate is an obvious possibility. These rates of uplift explain the overall profile of the Coastal Range as shown in Figure 10b; the resemblance implies that the patterns of short-term and long-term rates of uplifting of the Coastal Range may be similar.

[35] The decreasing uplift rate in northern Coastal Range is not the result of mimicking the shape of the subduction boundary however. If the shape of subduction/collision boundary is stationary, then continued compression should still result in shortening and mountain building, even after the plate begins to bend downward. The lower uplift rate in northern Coastal Range is probably controlled by the southward propagation of the Ryukyu Trench as a result of continued opening of the Okinawa Trough, whereby plate flexure occurs because of the increasing load.

4.4. Hoping Basin

[36] The Hoping Basin just offshore of NE Taiwan is a very peculiar structure (Figures 1 and 11). It has an N-S elongation and a very well delineated free-air gravity anomaly of about −230 mg [*Hsu et al.*, 1998] (Figure 11). This anomaly is apparently related to a deep sedimentary basin, with thickness of sediments estimated from wide-angle reflection data to be 10–15 km [*Hetland and Wu*, 2001;

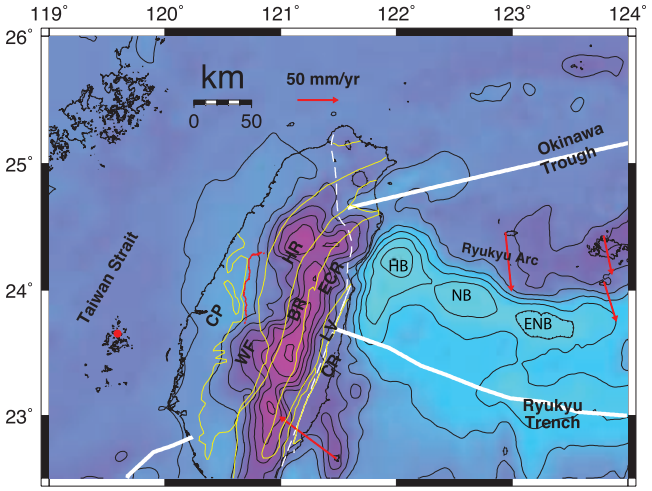

Figure 11. Free-air gravity anomaly map of Taiwan, showing the large negative anomaly over the Hoping Basin (HB). It is apparently related to the presence of deep sediments in the basin. Labels are explained in the caption for Figure 1a.

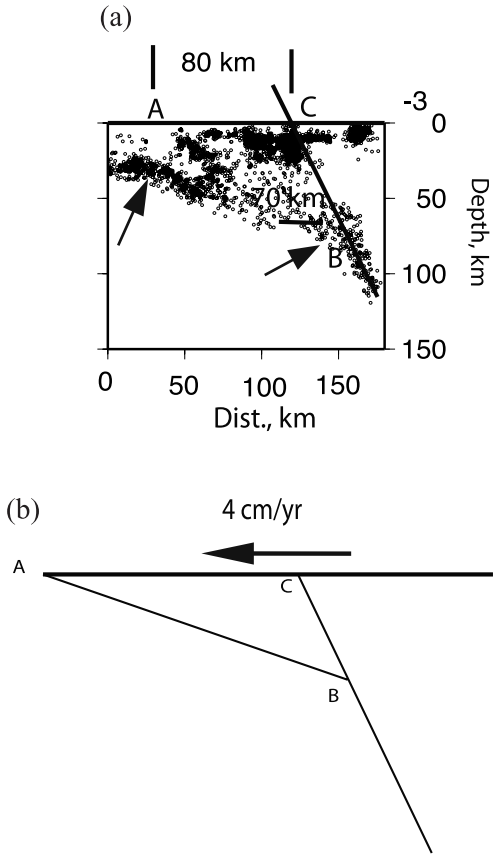

Figure 12. (a) Profile 9 from Figure 2b is shown here with the interpretation of the two segments of dipping seismic zone. (b) A simplified diagram indicates the relation between the spreading of the Okinawa Trough and the formation of the kink in the PSP slab. Before the opening of the trough, PSP subducts at a high angle. As the spreading continues, the wedge over PSP grows and the trench propagates to the left (or southward) and thus rolls the PSP forward to form a shallow dipping shallow dipping subduction zone on top. See discussion in the text.

McIntosh et al., 2005]. Some normal faults are exposed at the top of the basin sediments [*Font et al.*, 2001] and focal mechanisms of a series of recent earthquakes show normal faulting on the west and northwest side of the basin (Figure 6b). It is located at the foot of the Ryukyu Arc near, but isolated from, the Ilan Plain and Okinawa Trough (Figures 1 and 6b). On the west side a sheer cliff borders it, and the basin is dissected by faults [*Lallemand et al.*, 1997]. In our model the basin and NE Taiwan are on EUP with PSP subducting beneath. Both sides are on EUP; however, this area is likely to be under nearly E-W directed tension because of the differential motion on the two sides as explained earlier. The mechanism for the formation of the deep basin is an important problem. We hypothesize here that the continued WNW-ESE tension in this region led to the formation of this basin.

5. Discussion

[37] Two subduction zones with different polarities bracket Taiwan and both of them terminate under Taiwan. The southern zone is the northern extension of the Luzon subduction system [e.g., *Wu et al.*, 1997], and the northern one is the western extension of the Ryukyu system. The collision of the Luzon Arc with the Eurasian plate created Taiwan, and it is the northern zone that is involved in this collision. In this paper we are concerned particularly with the geometry and the kinematics of the subduction and collision boundaries and some of the associated collision processes of the northern zone. We have shown that the three segments, the LV, the collision/subduction boundary north of LV and the EUR/PSP subduction boundary, form a triple junction. The junction is located beneath the middle northern Longitudinal Valley. In reality this is not a point, and neither is the continuation of the subduction boundary on land a line; with continental materials involved on both side of the boundary near the junction we may expect complex changes in terms of crustal deformation in the vicinity. In section 4 we discuss the observations consistent with the junction model we have proposed. One additional aspect of this model is that PSP continues to advance westward when it enters the asthenosphere about 60 km below the surface as shown in Figure 5 and in an animated display in the Auxiliary Materials.

[38] The subduction indenter model we proposed is a dynamically changing one because of the active spreading of the Okinawa Trough. Currently the Ryukyu arc is moving nearly southward with respect to Penghu and at a velocity of more than 5 cm/a (Figure 1a), although the average velocity in the last 2 Ma or so was considerably less at 1.5 cm/a [*Sibuet et al.*, 1998]. At either velocity the ''trench'' will propagate southward. The propagation of the trench may add load to PSP near the trench and thereby depress the topography of the northern Coastal Range as suggested earlier.

[39] Additionally, it may also create the kink in the subduction zone (Figure 2b). *Scholz and Campos* [1995] [see also *Chase*, 1978; *Wu*, 1978; *Uyeda and Kanamori*, 1979] presented a model of subduction as a function of the absolute motion (say, in the hot spot framework) of the plates in question. In their ''passive mantle'' or the ''anchored slab'' model, a subducted slab in the upper mantle is held essentially fixed because of the resistance to motion perpendicular to the strike of the trench, with its dip controlled by the absolute motion of the nonsubducting upper plate. In case of the northern Taiwan slab, it had an initial dip of about 60° (as shown in Figure 12a), but when the Okinawa Trough began to open the motion of the upper plate changed, and at the same time the slab continued to descend at a rate determined by the slab pull, then a new slope for the shallow part of the slab was established, in accordance with the velocity of the upper plate (Figure 12b) and descending velocity of the steep part of the slab. In Figure 12a, the total distance of propagation is estimated to be about 80 km, roughly the same as the width of the Okinawa Trough [*Sibuet et al.*, 1998], and during the time the steep segment has descended about 70 km from C to B in Figure 12b. The propagation creates a time-dependent boundary condition for the orogeny and its effects may be discernible from dating structural evolution of the Central Range.

[40] Another alternative model of the ''kink'' was proposed by *Chou et al.* [2006]. They used a similar

combination of CWB and JMA data set as we have and found that the slab to the west of about 122.2°E defined by seismicity deeper than 50 km assumes a noticeable different trend from that to the east of 122.2°E. The part that is shown to bend (toward the north) is where we locate the kink. *Chou et al.* [2006] interpreted this bend to be the result of lateral compression of the PSP when it encounters the EUR lithosphere on its WNW path. That the end of PSP moves westward against a EUR agrees generally with our plate model and it is reasonable that it may have contributed toward the change in shape of the WBZ near Taiwan.

[41] The kind of triple junction described in this paper is not very common, although the eastern syntaxis of the Himalaya joining the Indian-Eurasian collision and the Myanmar subduction zone is a prominent example. This junction can be viewed as an advanced case of the northern Taiwan junction; it has gone on for so long that a giant geological bight and a whole series of surface structures have been created.

[42] In this study LV is considered the major boundary between PSP and EUP. Recent large earthquakes in the vicinity of LV have mostly been thrust events [*Wu et al.*, 1997]. An earthquake on 1 April 2006 showed that the displacement of the southern end of LV can be represented by partitioned left lateral and thrust [*Wu et al.*, 2006]. Together with the two major oblique-slip events in 1951 in the northern and the central of the valley [*Lee et al.*, 1998] it is very likely that LV is indeed the main boundary between PSP and EU in the collision section of Taiwan.

[43] There are many other aspects of the northern Taiwan subduction system that awaits further elucidation. For example, is the subducting part of the collision/subduction boundary capable of generating major earthquakes? The interface between EUR and PSP under Taiwan is currently a very active area and can perhaps be considered a potential source zone. Being under the land area and close to large metropolitan areas it is a zone worth watching.

6. Conclusion

[44] We present a model of 3-D architecture of the intersection of the Philippine Sea plate with the Eurasian plate in northern Taiwan based on seismicity and P wave tomography. We also show that other observations on land and offshore are consistent with the model. In this model the Ryukyu subduction plate boundary intersects Taiwan beneath the northern Coastal Range at about 23.7°N; north of this latitude the Coastal Range overlies the shallow dipping subducting zone. South of the intersection, the collision of the Philippine Sea plate with the Eurasian plate continues from the surface downward, but toward the north the collision occurs at successively greater depth as PSP subducts and persists in its northwestward motion. While the northwestward motion of PSP leads to its collision with the Eurasian plate, the locus of collision follows the geometry of the subduction zone. Above the inclined subduction zone at the shallow crust is a region of E-W tension because the Eurasian side of the boundary is still being shortened by the collision below, while the Eurasian plate above the subducting PSP is only loosely coupled to the PSP and does not follow PSP. In this scenario, EUP above the subducting PSP does not move in synch with the Taiwan EUP in front and thus creating a chance to develop E-W tension. Furthermore, as the subduction zone goes below about 50–60 km, the PSP enters into asthenosphere, whereby PSP is no longer colliding with the EUP lithosphere. If the Okinawa Trough continues to expand, the triple junction, as well as the Ryukyu subduction boundary near Taiwan, will continue to migrate southward. Thus, the three segments form a dynamic triple junction of subduction-collision-subduction/collision/separation. In order to understand the collision dynamics that produced Taiwan a detailed knowledge of the 3-D geometry of the boundary is critically needed.

[45] **Acknowledgments.** Assistance in ANSYS and GIS modeling by En-Jui Lee and Hao Kuo-Chen of SUNY Binghamton is greatly appreciated. Joint research with Long-Chen Kuo on continuous GPS data in Taiwan is beneficial for understanding the tectonics of this area. We also would like to thank Rich Briggs and Gavin Hayes of USGS for their careful reading and constructive comments on the manuscript. Yosio Nakamura's comments on any early draft were most helpful. NSF EAR-0410227 (F.T.W.) supports this research.

References

Angelier, J. (1986), Preface, *Tectonophysics*, *125*, IX–X, doi:101016/0040-1951(86)90003-X.

Angelier, J., F. Bergerat, H. T. Chu, and T. Q. Lee (1990), Tectonic analyses and the evolution of a curved collision belt: The Hsiiehshan Range, northern Taiwan, *Tectonophysics*, *183*, 77–96, doi:10.1016/0040-1951(90)90189-F.

Angelier, J., T.-Y. Chang, J.-C. Hu, C.-P. Chang, L. Siame, J.-C. Lee, B. Deffontaines, H.-T. Chu, and C.-Y. Lu (2009), Does extrusion occur at both tips of the Taiwan collision belt? Insights from active deformation studies in the Ilan Plain and Pingtung Plain regions, *Tectonophysics*, *466*, 356–376, doi:10.1016/j.tecto.2007.11.015.

Benz, H. M., B. A. Chouet, P. B. Dawson, J. C. Lahr, R. A. Page, and J. A. Hole (1996), Three-dimensional P and S wave velocity structure of Redoubt Volcano, Alaska, *J. Geophys. Res.*, *101*, 8111–8128, doi:10.1029/95JB03046.

Chase, C. G. (1978), Extension behind island arcs and motions relative to hot spots, *J. Geophys. Res.*, *83*, 5385–5387, doi:10.1029/JB083iB11p05385.

Chemenda, A. I., R.-K. Yang, J.-F. Stephan, E. A. Konstantinovskaya, and G. M. Ivanov (2001), New results from physical modeling of arc-continent collision in Taiwan: Evolutionary model, *Tectonophysics*, *333*, 159–178, doi:10.1016/S0040-1951(00)00273-0.

Chen, W. P., and C. Y. Chen (2004), Seismogenic structures along continental convergent zones: From oblique subduction to mature collision, *Tectonophysics*, *385*, 105–120, doi:10.1016/j.tecto.2004.04.022.

Chou, H.-C., B.-Y. Kuo, S.-H. Hung, L.-Y. Chiao, D. Zhao, and Y.-M. Wu (2006), The Taiwan-Ryukyu subduction-collision complex: Folding of a viscoelastic slab and the double seismic zone, *J. Geophys. Res.*, *111*, B04410, doi:10.1029/2005JB003822.

Deffontaines, B., O. Lacombe, J. Angelier, H. T. Chu, F. Mouthereau, C. T. Lee, J. Deramond, J. F. Lee, M. S. Yu, and P. M. Liew (1997), Quaternary transfer faulting in the Taiwan Foothills: Evidence from a multisource approach, *Tectonophysics*, *274*, 61–82, doi:10.1016/S0040-1951(96)00298-3.

Dominguez, S. S., S. Lallemand, J. Malavieille, and P. Schnürle (1998), Oblique subduction of the Gagua Ridge beneath the Ryukyu accretionary wedge system: Insights from marine observations and sandbox experiments, *Mar. Geophys. Res.*, *20*, 383–402, doi:10.1023/A:1004614506345.

Font, Y., C. S. Liu, P. Schnurle, and S. Lallemand (2001), Constraints on backstop geometry of the southwest Rhykyu subduction based on reflection seismic data, *Tectonophysics*, *333*, 135–158, doi:10.1016/S0040-1951(00)00272-9.

Font, Y., H. Kao, S. Lallemand, C. S. Liu, and L. Y. Chiao (2004), Hypocentre determination offshore of eastern Taiwan using the Maximum Intersection method, *Geophys. J. Int.*, *158*, 655–675, doi:10.1111/j.1365-246X.2004.02317.x.

Frohlich, C. (2001), Display and quantitative assessment of distribution of earthquake focal mechanisms, *Geophys. J. Int.*, *144*, 300–308, doi:10.1046/j.1365-246x.2001.00341.x.

Hetland, E. A., and F. T. Wu (2001), Crustal structure at the intersection of the Ryukyu Trench with the arc-continent collision in Taiwan; results

from an offshore-onshore seismic experiment, *Terr. Atmos. Oceanic Sci.*, *12*, 231–248.

Ho, C. S. (1988), An introduction to the geology of Taiwan: Explanatory text of the geologic map of Taiwan, Cent. Geol. Surv., Minist. of Econ. Affairs, Taipei, Taiwan.

Hsieh, M.-L., P.-M. Liew, and M.-Y. Hsu (2004), Holocene tectonic uplift on the Hua-tung coast, eastern Taiwan, *Quat. Int.*, *115–116*, 47–70, doi:10.1016/S1040-6182(03)00096-X.

Hsu, S. K., C. S. Liu, C. T. Shyu, S. Y. Liu, J. C. Sibuet, S. Lallemand, C. Wang, and D. Reed (1998), New gravity and magnetic anomaly maps in the Taiwan-Luzon region and their preliminary interpretation, *Terr. Atmos. Oceanic Sci.*, *9*, 509–532.

Hsu, Y. J., S. B. Yu, M. Simons, L. C. Kuo, and H. Y. Chen (2009), Interseismic crustal deformation in the Taiwan plate boundary zone revealed by GPS observations, seismicity, and earthquake focal mechanisms, *Tectonophysics*, doi:10.1016/j.tecto.2008.11.016, in press.

Hu, J. C., J. Angelier, and S. B. Yu (1997), An interpretation of the active deformation of southern Taiwan based on numerical simulation and GPS studies, *Tectonophysics*, *274*, 145–169, doi:10.1016/S0040-1951(96)00302-2.

Iidaka, T., M. Mizouie, and K. Suyehiro (1992), Seismic velocity structure of the subducting Pacific Plate in the Izu-Bonin region, *J. Geophys. Res.*, *97*, 15,307–15,319, doi:10.1029/92JB01336.

Kao, H., and P. R. Jian (2001), Seismogenic patterns in the Taiwan region: Insights from source parameter inversion of BATS data, 2001, *Tectonophysics*, *333*, 179–198, doi:10.1016/S0040-1951(00)00274-2.

Kao, H., and R. J. Rau (1999), Detailed structures of the subducted Philippine sea plate beneath northeast Taiwan: A new type of double seismic zone, *J. Geophys. Res.*, *104*, 1015–1033, doi:10.1029/1998JB900010.

Kao, H., S.-S. J. Shen, and K. F. Ma (1998a), Transition from oblique subduction to collision: Earthquakes in the southernmost Ryukyu arc-Taiwan region, *J. Geophys. Res.*, *103*, 7211–7229, doi:10.1029/97JB03510.

Kao, H., P.-R. Jian, K.-F. Ma, B.-S. Huang, and C.-C. Liu (1998b), Moment-tensor inversion for offshore earthquakes east of Taiwan and their implications to regional collision, *Geophys. Res. Lett.*, *25*, 3619–3622, doi:10.1029/98GL02803.

Lacombe, O., F. Mouthereau, J. Angelier, and B. Deffontianes (2001), Structural, geological and seismological evidence for tectonic escape in SW Taiwan, *Tectonophysics*, *333*, 323–345, doi:10.1016/S0040-1951(00)00281-X.

Lallemand, S. E., C. S. Liu, and Y. Font (1997), A tear fault boundary between the Taiwan orogen and the Ryukyu subduction zone, *Tectonophysics*, *274*, 171–190, doi:10.1016/S0040-1951(96)00303-4.

Lallemand, S. E., Y. Font, H. Bijwaard, and H. Kao (2001), New insights on 3-D plates interaction near Taiwan from tomography and tectonic implications, *Tectonophysics*, *335*, 229–253, doi:10.1016/S0040-1951(01)00071-3.

Lee, J.-C., J. Angelier, H.-T. Chu, S.-B. Yu, and J.-C. Hu (1998), Plate-boundary strain partitioning along the sinistral collision suture of the Philippine and Eurasian plates: Analysis of geodetic data and geological observation in southeastern Taiwan, *Tectonics*, *17*(6), 859–871, doi:10.1029/98TC02205.

Liang, W. T., Y. H. Liu, and H. Kao (2004), Source parameters of regional earthquakes in Taiwan: January-December, 2002, *Terr. Atmos. Oceanic Sci.*, *15*, 727–741.

Liew, P. M., P. A. Pirazzoli, M. L. Hsieh, M. Arnold, J. P. M. Fontugne, and P. Giresse (1993), Holocene tectonic uplift deduced from elevated shorelines, eastern Coastal Range of Taiwan, *Tectonophysics*, *222*, 55–68, doi:10.1016/0040-1951(93)90189-Q.

Liu, C. C., and S. B. Yu (1990), Vertical crustal movements in eastern Taiwan and their tectonic implications, *Tectonophysics*, *183*, 111–119, doi:10.1016/0040-1951(90)90191-A.

Lu, C. Y., J. Angelier, H. T. Chu, and J. C. Lee (1995), Contractional, transcurrent, rotational and extensional tectonics: Examples from northern Taiwan, *Tectonophysics*, *246*, 129–146, doi:10.1016/0040-1951(94)00252-5.

McIntosh, K., Y. Nakamura, T. K. Wang, R. C. Shih, A. C. Chen, and C.-S. Liu (2005), Crustal-scale seismic profiles across Taiwan and the western Philippine Sea, *Tectonophysics*, *401*, 23–54, doi:10.1016/j.tecto.2005.02.015.

Nakamura, M. (2004), Crustal deformation in the central and southern Ryukyu arc estimated from GPS data, *Earth Planet. Sci. Lett.*, *217*, 389–398, doi:10.1016/S0012-821X(03)00604-6.

Rau, R.-J., and F. T. Wu (1995), Tomographic imaging of lithospheric structures under *Taiwan*, *Earth Planet. Sci. Lett.*, *133*, 517–532, doi:10.1016/0012-821X(95)00076-O.

Rau, R.-J., K.-E. Ching, J.-C. Hu, and J.-C. Lee (2008), Crustal deformation and block kinematics in transition from collision to subduction: Global Positioning System measurements in northern Taiwan, 1995–2005, *J. Geophys. Res.*, *113*, B09404, doi:10.1029/2007JB005414.

Scholz, C. H., and J. Campos (1995), On the mechanism of seismic decoupling and back arc spreading at subduction zones, *J. Geophys. Res.*, *100*, 22,103–22,115, doi:10.1029/95JB01869.

Seno, T. (1977), The instantaneous rotation vector of the Philippine sea plate relative to the Eurasian plate, *Tectonophysics*, *42*, 209–226, doi:10.1016/0040-1951(77)90168-8.

Sibuet, J.-C., B. Defontaines, S. K. Hsu, N. Thareau, J. P. Le Formal, and C. S. Liu (1998), ACT party, Okinawa trough backarc basin: Early tectonic and magmatic evolution, *J. Geophys. Res.*, *103*, 30,245–30,267, doi:10.1029/98JB01823.

Sibuet, J.-C., S.-K. Hsu, X. Le Pichon, J.-P. Le Formal, D. Reed, G. Moore, and C.-S. Liu (2002), East Asia plate tectonics since 15 Ma: Constraints from the Taiwan region, *Tectonophysics*, *344*, 103–134, doi:10.1016/S0040-1951(01)00202-5.

Uyeda, S., and H. Kanamori (1979), Back-arc opening and the mode of subduction, *J. Geophys. Res.*, *84*, 1049–1061, doi:10.1029/JB084iB03p01049.

Waldhauser, F., and W. L. Ellsworth (2000), A double-difference earthquake location algorithm: Method and application to the northern Hayward Fault, California, *Bull. Seismol. Soc. Am.*, *90*, 1353–1368, doi:10.1785/0120000006.

Wu, F. T. (1978), Benioff zones, absolute motion and interarc basin, *J. Phys. Earth*, *26*, Supplement, S39–S54.

Wu, F. T., R. J. Rau, and D. Salzberg (1997), Taiwan orogeny: Thin-skinned or lithospheric collision, *Tectonophysics*, *274*, 191–220, doi:10.1016/S0040-1951(96)00304-6.

Wu, F. T., C. S. Chang, and Y. M. Wu (2004), Precisely relocated hypocenters, focal mechanisms and active orogeny in central Taiwan, in *Aspects of the Tectonic Evolution of China*, edited by J. Malpas et al., *Geol. Soc. Spec. Publ.*, *226*, 333–353.

Wu, F., L. C. Kuo, and H. Kuo-Chen (2007), Deformation of Taiwan from continuous GPS monitoring, *Eos Trans. AGU*, *88*(52), Fall Meet. Suppl., Abstract T42A-01.

Wu, Y.-M., Y.-G. Chen, C.-H. Chang, L.-H. Chung, T.-L. Teng, F. T. Wu, and C.-F. Wu (2006), Seismogenic structure in a tectonic suture zone: With new constraints from 2006 Mw6.1 Taitung earthquake, *Geophys. Res. Lett.*, *33*, L22305, doi:10.1029/2006GL027572.

Wu, Y.-M., C.-H. Chang, L. Zhao, J. B. H. Shyu, Y.-G. Chen, K. Sieh, and J.-P. Avouac (2007), Seismic tomography of Taiwan: Improved constraints from a dense network of strong motion stations, *J. Geophys. Res.*, *112*, B08312, doi:10.1029/2007JB004983.

Yamaguchi, M., and Y. Ota (2004), Tectonic interpretations of Holocene marine terraces, east coast of Coastal Range, Taiwan, *Quat. Int.*, *115–116*, 71–81, doi:10.1016/S1040-6182(03)00097-1.

Yu, S. B., and L. C. Kuo (2001), Present-day crustal motion along the Longitudinal Valley fault, eastern Taiwan, *Tectonophysics*, *333*, 199–217.

Yu, S. B., H. Y. Chen, and L. C. Kuo (1997), Velocity field of GPS stations in the Taiwan area, *Tectonophysics*, *274*, 41–59, doi:10.1016/S0040-1951(96)00297-1.

H. Benz, U.S. Geological Survey, MS 966, P.O. Box 25046, Denver, CO 80225-0046, USA.

J.-C. Lee and W.-T. Liang, Institute of Earth Sciences, Academia Sinica, P.O. Box 1-55, Nankang, Taipei 11529, Taiwan.

A. Villasenor, Instituto de Ciencias de la Tierra "Jaume Almera," CSIC, c/ Lluís Solé i Sabarís s/n, E-08028 Barcelona, Spain.

F. T. Wu, Department of Geological Sciences, State University of New York at Binghamton, Binghamton, NY 13902, USA. (francis@binghamton.edu)